Biochimica et Biophysica Acta 897 (1987) 384–394
Elsevier

BBA 73375

Fluorescent labeling of bacteriorhodopsin: implications for helix connections

Robert Renthal [a,b], Marian Cothran [a], Nancy Dawson [a] and Gary J. Harris [a,*]

[a] *Division of Earth and Physical Sciences, The University of Texas at San Antonio, San Antonio, TX and* [b] *Department of Biochemistry, The University of Texas Health Science Center at San Antonio, San Antonio, TX (U.S.A.)*

(Received 19 May 1986)
(Revised mansucript received 18 November 1986)

Key words: Bacteriorhodopsin; Purple membrane; Proton pump; Fluorescence energy transfer; Membrane protein conformation; (*H. halobium*)

Purple membrane from *Halobacterium halobium* was reacted with dansyl (5-dimethylamino-1-naphthalenyl) fluorescent labels that have specificity for different protein side chains of bacteriorhodopsin. Dansyl chloride was found to react primarily with Lys-41. Dansyl hydrazine was coupled, with water-soluble carbodiimide, to Glu-74 and/or Asp-85, which was the major modified site after papain-cleavage of the carboxyl-terminal 17 amino acids. Fluorescence energy transfer was used to probe the proximity of the modified sites to the retinal chromophore of bacteriorhodopsin. The dansyl group on Lys-41 was greater than 2.99 nm from retinal, while the dansyl group on Glu-74/Asp-85 was greater than 2.10 nm from retinal. Information available on the location of retinal in the transmembrane profile and probable surface locations of the fluorescent labels was combined with the energy transfer results to calculate distances projected in the plane of the membrane. The projected distances to retinal were 1.64 nm (Lys-41) and 1.65 nm (Gly-74). These measurements, combined with many other labeling experiments that have been reported, restrict the number of likely helix-connection models to only three: EDCABGF, FEDCBAG and FGEABDC (in the nomenclature of Engelman et al. (1980) Proc. Natl. Acad. Sci. USA 77, 2023–2027).

Introduction

Purple membrane from *Halobacterium halobium* contains the light-induced proton pump bacteriorhodopsin to which the chromophore all-*trans* retinal is linked at Lys-216 as a Schiff base (see Ref. 1 for a recent review). Image reconstruction from low-dose electron micrographs [2] revealed that the structure of bacteriorhodopsin at low resolution consists of seven cylindrical electron-dense regions, presumably α-helices, roughly perpendicular to the plane of the membrane. The connections between these helices and the identification of the helices with particular segments of the bacteriorhodopsin amino acid sequence have been the object of numerous studies (for example, Refs. 3–10). No consensus has yet emerged. Indeed, some results contradict the general assumption of an entirely α-helical structure [11].

Previous experiments in this laboratory resulted in several apparently specific fluorescent labeling reactions [12,13]. We have now localized the amino

* Present address: Department of Surgery, The University of Iowa Hospitals and Clinics, Iowa City, IA 52242, U.S.A.

Abbreviations: HFBA, heptafluorobutyric acid; EDC, 1-ethyl-3-(3-dimethylaminopropyl)carbodiimide; 1,8-ANS, 1-anilinonaphthalene-8-sulfonic acid; dansyl, [5-(dimethylamino)-1-naphthalenyl]sulfonyl; CT1, bacteriorhodopsin chymotrypsin fragment containing residues 72–248; PTH, phenylthiohydantoin.

Correspondence: R. Renthal, Division of Earth and Physical Sciences, The University of Texas at San Antonio, San Antonio, TX 78285, U.S.A.

acid sequence positions of these labels with the objective of measuring dipole resonance energy transfer between the labels and retinal, the purple chromophore of bacteriorhodopsin [14,15]. The energy transfer efficiency to retinal of a particular amino acid sequence position could serve as a useful additional constraint for attempts at helix connection model building.

Experimental methods

Isolation of purple membrane. Purple membrane was prepared from *H. halobium* S9 as described by Oesterhelt and Stoeckenius [16].

Reaction of purple membrane with dansyl chloride. This reaction was performed as previously described [12] except that the dansyl chloride stock solution to be added to the reaction mixture was first mixed with a residue of [^{3}H]dansyl chloride (New England Nuclear) dried from pentane, which contained the desired level of radioactivity.

Purification of dansyl chloride-labeled peptide. Cleavage with chymotrypsin, purification by LH-60 chromatography, cleavage with CNBr, and purification by LH-20 chromatography were performed as previously described [17,12]. Protein concentration was measured by acid hydrolysis (6 M HCl, 24 h, 110°C) followed by analysis on a Durrum 500 amino acid analyzer. Radioactivity was measured by liquid scintillation counting in Aquasol II (New England Nuclear). Amino acid sequence analysis was performed on a Beckman 890C Sequencer, using a 0.1 M quadrol program. Anilino thiazalinone amino acids were converted to phenylthiohydantoins (PTH) in 1 M aqueous HCl and the products were analyzed by HPLC.

Purification of non-protein-bound label. Lipids were extracted from dansyl chloride-labeled purple membrane by the method of Bligh and Dyer [18] and separated on a 0.25 mm silica 60 thin layer plate (E. Merck) in $CHCl_3$/80% acetic acid/methanol 30 : 10 : 4. After observing the fluorescence pattern under ultraviolet light, the plate was stained for phospholipids with molybdate [19].

Lipids were also separated from bacteriorhodopsin on an agarose gel column as described by Huang et al. [20].

Functional characterization of dansyl-Lys-41-bacteriorhodopsin: rate of regeneration. Purple membrane sheets (20 nmol bacteriorhodopsin or dansyl-Lys-41-bacteriorhodopsin) were suspended in 2 ml hydroxylamine (0.16 M final concentration, pH 7.0) and illuminated for 45 min, with a projector lamp, to form retinal oxime. The membranes were washed by centrifugation three times, with resuspension first in 0.05 M NaCl, then 0.015 M NaCl and finally 2 ml of water. The regeneration reaction was started by addition of 5 μl of 4.5 mM all-*trans* retinal in ethanol. Absorbance changes at 570 nm were followed as a function of time on a Beckman Acta spectrophotometer.

Photoreaction cycle. Rates of formation and decay of photointermediates L, M and O of dansyl-Lys-41-purple membrane sheets were measured by flash spectroscopy using the apparatus constructed by Lozier et al. [21] with the generous assistance of R. Bogomolni, University of California at San Francisco.

Reaction of purple membrane with dansyl hydrazine and characterization of product. This reaction was done as previously described [13] except that the published procedure contains a typographic error (12 ml of solution B was added to solution A, not 4.8 ml). Papain cleavage of dansyl-hydrazine-labeled membrane with papain was also performed as described [13], using a larger-scale reaction. The product was monitored by gel electrophoresis to verify removal of the C-terminal peptide. Reaction of the papain-cleaved dansyl-hydrazine-labeled membrane with chymotrypsin followed the procedure described by Gerber et al. [17]. Cleavage with CNBr at Met residues was done following the procedure of Gerber et al. [17]. Cleavage at both Met and Trp was done as follows. Approximately 300–500 nmol of papain-cleaved dansyl-hydrazine-labeled membrane was lyophilized, dissolved in 3 ml 88% formic acid, diluted with 7 ml of ethanol and applied to a 2.5×90 cm column of LH-60 (Pharmacia) equilibrated with formic acid/ethanol 30 : 70. The material eluting in the void volume, containing lipid-free protein, was evaporated under reduced pressure. The residue was dissolved in 3 ml 88% formic acid, diluted with 3 ml anhydrous heptafluorobutyric acid (HFBA), and added to 2.1 g CNBr [22]. After 24 h, the solvent was partially evaporated under a stream of N_2 and the remainder was diluted with approximately 10 ml

water ad lyophilized. Chromatography of the CNBr peptides was performed on LH-60 as described by Khorana et al. [23], and the peptides were further purified on a Bio-Rad C_{18} column (4.8–250 mm) [17].

Functional characterization of dansyl-Glu-74/Asp-85-bacteriorhodopsin. Purple membrane was reacted with 1-ethyl-3-(3-dimethylaminopropyl)-carbodiimide (EDC) as previously described [24], for 1 h, using various concentrations of EDC. Light-induced changes in H^+ binding were measured on the products at pH 9.0 [25]. Purple membrane that had been reacted with a 210:1 molar ratio of EDC to bacteriorhodopsin was subsequently reacted with [^{3}H]dansyl hydrazine, as described above. The extent of incorporation of label was measured as previously described [13].

Fluorescence spectroscopy. Steady-state fluorescence emission spectra were measured on a Farrand MKI fluorometer with a ratio recording accessory. Static fluorescence polarization and fluorescence emission kinetics were measured as previously described [13].

The emission of the Farrand fluorometer was corrected using 1-anilinonaphthalene-8-sulfonic acid (1,8-ANS) in ethanol [26] and quinine sulfate in 0.1 M H_2SO_4 [27]. Purple membrane that had been reacted with dansyl chloride or dansyl hydrazine was washed five times with 0.05 M Tris (pH 8) for dansyl chloride, or four times with dilute NaCl and once with water for dansyl hydrazine, and resuspended in water at a concentration of 10^{-4} M bacteriorhodopsin. The dansyl membrane (0.70 ml) was then dissolved in 0.8% Triton X-100 (0.70 ml) for several hours at room temperature and diluted with 2.6 ml of 0.4% Triton X-100. half of the sample was then bleached by adjustment to pH 2.1 with HCl. After measuring the absorbance spectrum, the pH was brought back to 6.8 with 1 M NaOH. Bleached and unbleached samples were diluted 1:4 in 0.4% Triton X-100 and fluorescence emission spectra were measured. Quantum yields were calculated with reference to 1,8-ANS or quinine sulfate.

Results

Location of the dansyl chloride site

Purple membrane was labeled with [^{3}H]dansyl chloride in order to locate the sequence position of the dansyl label and to measure the amount of non-covalently bound dansyl group associated with intact membranes after the labeling reaction.

The yields of the steps in the reaction used for sequence analysis are shown in Table I. The purification of the labeled peptide is exactly as previously reported [12] except the HPLC purification step was omitted, since the contaminating peptide in the LH-20 fractions used for sequence analysis, CNBr 2, has a blocked N-terminus. Sequential Edman degradation of CNBr 1 (Fig. 1) shows label exclusively at position 9, which corresponds to Lys-41. No significant label is released at position 8 (Lys-40) or position 11 (Tyr-43). Thus, the dansyl chloride labeling reaction appears to be exclusively at Lys-41.

After labeling purple membrane with dansyl chloride, we previously found approximately 2 mol of dansyl per mol of bacteriorhodopsin [12]. Since only one modified site was found on the protein, we assumed that the additional label represented lipid-associated label. Thin-layer chromatography of the extracted dansyl purple membrane lipid showed that most of the non-protein label is not dansic acid. Two major yellow-fluorescent dansyl spots migrated in the region of the sulfated lipids, but the lipid composition and distribution did not appear altered by dansylation. Chromatography of deoxycholate-solubilized dansyl purple membrane on agarose showed that 75% of the label migrated with bacteriorhodopsin and 25% with the lipids. The average labeling stoichiometry of the lipid-free bacteriorhodopsin fractions after gel filtration was 1.3 ± 0.4 mol of dansyl per mol of bacteriorhodopsin (three measurements). The presence of non-protein-bound label could interfere with use of the labeled membrane for fluorescence spectroscopy. However, we found that incubation of the labeled membrane in 0.05 M Tris (pH 8.0) at 37°C for 1 h followed by centrifugation and resuspension removed 18% of the label. Samples used for spectroscopy were repeatedly washed with Tris until a non-fluorescent supernatant was obtained.

Functional properties of dansyl-Lys-41-bacteriorhodopsin

Some functional properties of dansyl-Lys-41-

TABLE I

YIELDS OF DANSYL-BACTERIORHODOPSIN AND DANSYL PEPTIDES

n.d., not determined; p, on basis of recovered peptide; c, on basis of recovered counts; r, repetitive yield.

Sample	Total cpm	mol dansyl	mol bacterio-rhodopsin or peptide	mol dansyl/ mol bacterio-rhodopsin or peptide	Percent yield from previous step
1. Reaction mixture	$2.74 \cdot 10^7$	48.1 μmol	1.2 μmol	–	–
2. Dansyl-bacteriorhodopsin	$1.46 \cdot 10^6$	2.56 μmol	0.95 μmol	2.6	79 (p)
3. Chymotrypsin-cleaved dansyl-bacteriorhodopsin	663000	1.16 μmol	n.d.	–	45 (c)
4. Dansyl-CT2	370000	648 nmol	n.d.	–	56 (c)
pooled fractions	209000	367 nmol	417 nmol	0.88	–
5. Dansyl-CNBr1	157000	275 nmol	n.d.	–	75 (c)
applied to sequenator	68600	120 nmol	n.d.	–	–
6. Sequence, round 9	3100	5.45 nmol	7 nmol	0.8	70 (r)
recovered from sequenator after round 12	10900	19.2 nmol	n.d.	–	–

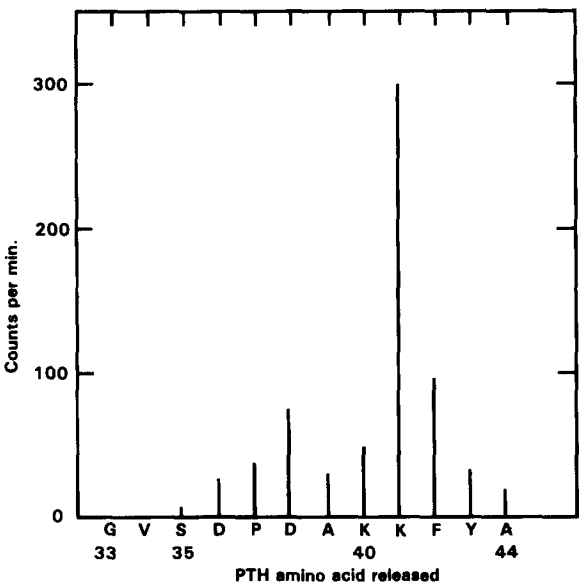

Fig. 1. Sequence analysis of dansyl chloride-modified peptide. A mixture of CNBr fragments 33–56 and 1–20 were applied to a Beckman 890 sequenator [17]. The dried PTH amino acid fractions were each solubilized in 1 ml ethyl acetate; 0.1 ml was withdrawn and added to 10 ml Aquasol-2 for liquid scintillation counting. PTH amino acids identified by HPLC in each Edman round are given on the abscissa with the one-letter amino acid code.

bacteriorhodopsin in addition to those previously reported [12] were examined. The rate of regeneration of the 570 nm chromophore with all-*trans* retinal after NH_2OH bleaching was found to be indistinguishable from unmodified purple membrane (Table II). Furthermore, the photoreaction cycle was essentially the same as that of the unmodified membrane (although a small inhibition of the decay of O was noted; data not shown).

Location of the internal dansyl hydrazine site

Purple membrane was reacted with dansyl hydrazine in the presence of EDC, followed by enzymatic and chemical cleavage in order to locate the sequence position of the modification. Papain treatment released more than half the dansyl hydrazine label. We previously presented evidence that the dansyl hydrazine sites released by papain are on the carboxyl-terminal tail [13]. The remaining label migrated with the large chymotryptic fragment (CT1) on LH-60 chromatography (Fig. 2). The hydrazide linkage appeared to be somewhat unstable in light and acid and variable amounts of the label were cleaved, apparently during dissolution is concentrated formic acid prior to LH-60 chromatography. Reaction of

TABLE II

REGENERATION OF PURPLE CHROMOPHORE WITH ALL-*TRANS* RETINAL

Time (s)	Percent regeneration	
	bacterio-rhodopsin	dansyl-Lys-41-bacteriorhodopsin
0	0	0
100	72	60
400	100	98
1150	100	100

papain-cleaved CT1 with CNBr, followed by reverse phase HPLC separation (Fig. 3), showed that the yield of material peaking at fraction 55, CNBr 10 (residues 72–118), was diminished compared to control experiments [17] while the yields of CNBr 9 (residues 163–209) and CNBr 7 (residues 119–145) were unaltered. (Yields were estimated by relative ultraviolet absorbance.) Two additional peptides do not show up on the reverse phase chromatogram, and they were examined by LH-60 chromatography of the same mixture of

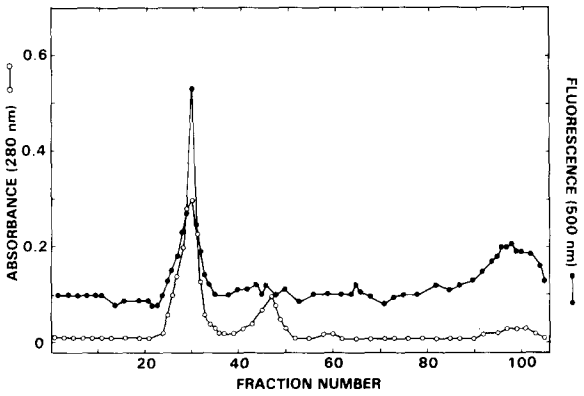

Fig. 2. Separation of chymotrypsin fragments of dansyl-hydrazine-modified bacteriorhodopsin. Fluorescent-labeled protein was cleaved first with papain [13] and then with chymotrypsin [17]. The fragments were separated by gel filtration on a column of LH-60 (2.5×90 cm) in 88% formic acid/ethanol 30:70. Fractions of 4 ml were collected. Absorbance at 280 nm and fluroescence at 500 nm (excitation = 330 nm) were monitored. Approximately 60% of the label migrates with the large chymotrypsin fragment (fractions 23–32, containing residues 72–248), 0% with the small fragment (fractions 41–50, containing residues 1–71) and 40% in the included volume (fractions 91–105, containing retinal, lipids and free label).

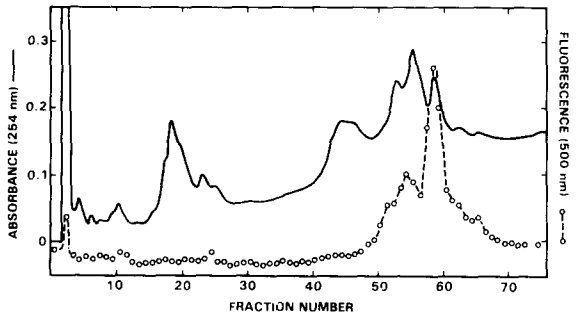

Fig. 3. Separation of CNBr fragments from residues 72–231 of dansyl-hydrazine-modified bacteriorhodopsin: cleavage at methionine. The large chymotrypsin fragment of dansyl-hydrazine-modified bacteriorhodopsin was cleaved with CNBr and applied to a C_{18} reverse-phase column [17]. The sample was applied in 88% formic acid and eluted with a gradient from 40% to 80% of ethanol in water. Mobile phase contained 5% formic acid. Fractions of 1 ml were collected. Absorbance (254 nm) and fluorescence (500 nm, excitation at 330 nm) were monitored.

CNBr fragments [23]. No fluorescence migrated with peptides in the 2000 molecular weight range (data not shown), ruling out modification of papain-cleaved CNBr 6 (residues 209–231) and CNBr 11 (residues 146–163). Thus, after dansyl hydrazine labeling and papain cleavage, only CNBr 10 appears to be modified. This peptide contains six potential dansyl hydrazine modification sites: Glu-74, Asp-85, Asp-96, Asp-102, Asp-104, and Asp-115. Further localization of the site was simplified by the fortuitous arrangement of tryptophan residues at position 80 (between Glu-74 and Asp-85) and position 86 (between Asp-85 and Asp-96). The CNBr cleavage method of Ozols and Gerard [22] proved to be a satisfactory method of scission at Trp, as we recently reported [28]. Despite the high (3.5 molal) CNBr concentration, the fluorescence properties of the dansyl group appeared unaltered. The chymotrypsin cleavage step was omitted for convenience. Whole, lipid-free dansyl-hydrazine-labeled, papain-treated bacteriorhodopsin was cleaved at both Trp and Met by CNBr in 1:1 heptafluorobutyric acid/88% formic acid. The resulting fragments were separated by LH-60 chromatography (Fig. 4). Fractions 83–100 were shown to be dansic acid by fluorescence emission and thin layer chromatography. Two major peaks were observed at fractions 70 and 77,

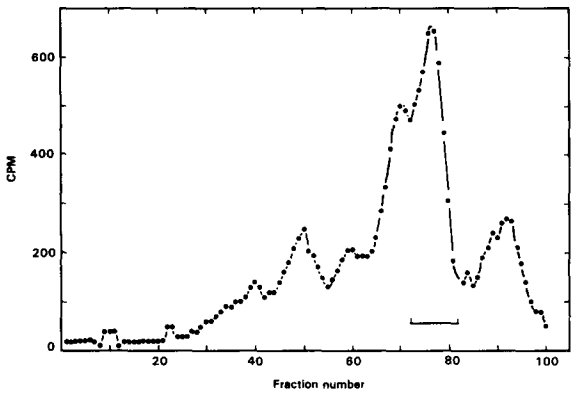

Fig. 4. Separation of CNBr fragments of dansyl-hydrazine-modified bacteriorhodopsin: cleavage at methionine and tryptophan. Bacteriorhodopsin was labeled with [^{3}H]dansyl hydrazine and then cleaved with papain. The modified protein was reacted with CNBr in heptafluorobutyric acid/88% formic acid 1:1 to cleave at both methionine and tryptophan. The mixture of peptides was separated on an LH-60 gel filtration column as described in Fig. 2. A 0.1 ml sample of each fraction was examined for ^{3}H by liquid scintillation counting.

with minor peaks at 40, 50 and 60. Calibration of the gel filtration column was done with Met cleavage CNBr fragments of bacteriorhodopsin [17] which migrate according to molecular size when chromatographed after treatment with perfluorocarboxylic acids [23]. Peptides of approximately 5000 molecular weight elute with a peak at fraction 55, while fragments of approximately 3000 molecular weight elute with a peak at fraction 65. Since no CNBr fragment can migrate with a peak prior to fraction 55, the radioactivity in the fractions with peaks at 40 and 50 must represent partial cleavage products. Cleavage of CNBr 10 and Trp is expected to produce three fragments containing residues 69–80, 81–86 ad 87–118. The radioactivity in the peak at fraction 60 could represent label on the 87–118 fragment or partial cleavage products. The label in the peak at fractions 70 and 77 can only be due to label on residues 69–80 and/or 81–86. Of the label in CNBr fragments, 10.7% is in the peak at fraction 60, while 89.3% is in the peaks at fractions 70 and 77. Thus, most of the label is on Glu-74 and/or Asp-85. The yields of each step in the isolation of these peptides are shown in Table III.

Functional properties of dansyl-Glu-74/Asp-85-bacteriorhodopsin

Preliminary experiments [29] suggested that the internal dansyl hydrazine stie was the same as a site which can be modified at neutral pH by water-soluble carbodiimide, resulting in inhibition of the proton uptake step of the proton pump [24] and inhibition of the formation of the acid-induced blue pigment [30]. However, upon finding the fluorescent labeling site on the extracellular side of the membrane, we re-examined the apparent competition between carbodiimide modification and subsequent fluorescent labeling. We found that the water-soluble carbodiimide inhibition of proton uptake extends down to much lower concentrations than those previously used

TABLE III

YIELDS OF DANSYL HYDRAZINE-BACTERIORHODOPSIN AND DANSYL HYDRAZINE-PEPTIDES

n.d., not determined; p, on basis of peptide; c, on basis of counts.

Sample	total cpm [a]	Dansyl hydrazine (nmol)	Bacteriorhodopsin or peptide (nmol)	mol dansyl hydrazine/ mol bacteriorhodopsin or peptide	Percent yield from previous step
1. Reaction mixture	$1.4 \cdot 10^8$	40000	1000	–	–
2. Dansyl hydrazine-bacteriorhodopsin	(4320) [b]	(1.22) [b]	(1.07) [b]	1.1	–
3. Papain-cleaved dansyl-hydrazine-bacteriorhodopsin	$7.3 \cdot 10^5$	206	420	0.49	42 (p)
4. Low-M_r CNBr fragments	$5.0 \cdot 10^5$	142	n.d.	–	69 (c)

[a] Total yield at each step was applied to the next step. Total yield in step 2 was not determined.
[b] Measured from a small aliquot of the purified product from step 1.

(Table IV). At 3 mM EDC, the inhibition of proton uptake is over 80% of the maximum. However, after pre-reacting purple membrane with this concentration of EDC, the internal dansyl hydrazine site still can be labeled to the same extent as in unmodified membrane. Thus, the pump-inhibiting water-soluble carbodiimide site is not Glu-74/Asp-85. Our previous observation of partial inhibition of labeling of the internal dansyl hydrazine site was probably due to the aggregated state of purple membrane after treatment with high concentrations of carbodiimide.

Fluorescence energy transfer measurements

Dipole resonance energy transfer has been used to measure proximity between a fluorophore and a nearby chromophore that acts as a fluorescence energy acceptor [31]. Naphthalenesulfonyl fluorescent labels and retinal pigments are excellent energy donor-acceptor pairs [14,15]. Therefore, we examined the energy transfer characteristics of dansyl-Lys-41-bacteriorhodopsin in order to find out the label's proximity to retinal.

In order to avoid multiple-energy acceptors, labeled purple membrane was dissolved in Triton X-100, under conditions where there is only one bacteriorhodopsin per micelle [32]. The retinal chromophore environment, protein secondary structure, and light-induced proton release and uptake of bacteriorhodopsin are not drastically affected by the presence of Triton [11,33,34], suggesting no major structural alterations of the protein.

Corrected emission spectra of dansyl-Lys-41-bacterioopsin and dansyl-Lys-41-bacteriorhodopsin were measured and the fluorescence energy transfer efficiency was calculated as 0.74 (Table V). Decay of emission anisotropy from dansyl chloride-labeled purple membrane leveled off at constant anisotropy, in a manner similar to that reported for dansyl hydrazine attached at the carboxyl-terminal tail [13], and for other membrane probes [35]. Under these conditions, an estimate of the dipole orientation factor, K^2, may be made as follows. The energy acceptor is assumed to be completely fixed and rigid. The energy donor is assumed to have rotational freedom within a cone having its axis normal to the plane of the membrane. As shown by Kawato et al. [35], this angle, θ_c, may be calculated from the ratio of r, the anisotropy extrapolated to infinite time, to r_0, the limiting anisotropy. Because of light pulse and scattering artifacts, the value of r is not accurately measurable from our anisotropy decay kinetics data. However, the static anisotropy is approximately equal to r when the anisotropy decay is essentially flat after a brief, small rapid decline from the limiting value as in the present case. Thus, we have used static anisotropy data to estimate θ_c. The limiting anisotropy of 0.204 and a static anisotropy of 0.158 (at 23°C) imply a cone angle of 23°. According to the analysis by Stryer [31], this indicates a range of K^2 from 0.078 to 3.2. Based on measurements of donor quantum yield and donor-acceptor spectral overlap, we

TABLE IV

EDC INHIBITION OF PROTON PUMP ACTIVITY

EDC (mM)	Steady-state acidification (mequiv./mol) [a]
0	4
1	25
3	32
15	43
62	48

[a] Measured at pH 9.0 as described in Ref. 25.

TABLE V

SUMMARY OF FLUORESCENCE ENERGY TRANSFER PARAMETERS

	Dansyl-Lys-41	Dansyl-Glu-74/Asp-85
Quantum yield (no acceptor)	0.48	0.15
Quantum yield (acceptor present)	0.125	0.022
Transfer efficiency	0.74	0.85
Spectral overlap ($M^{-1} \cdot cm^3$)	$2.44 \cdot 10^{-13}$	$2.58 \cdot 10^{-13}$
Limiting anisotropy	0.204	0.285
Static anisotropy, 23°C	0.158	0.240
K^2	0.078–3.2	0.055–3.5
R_0 (nm)	3.6–6.6	2.8–5.6
Minimal distance, donor to retinal (nm)	2.99	2.10

estimate that the distance at 50% transfer, R_0, could range from 3.6 to 6.6 nm. Considering the parameters in Table V, the separation between dansyl-Lys-41 and retinal in bacteriorhodopsin must be between 2.99 and 5.5 nm.

An analysis of energy transfer similar to that described above was performed on the dansyl-Glu-74/Asp-85 site. Dansyl hydrazine-labeled membrane samples were cleaved with papain to remove the carboxyl-terminal tail, leaving only the Glu-74/Asp-85 site. These samples were then dissolved in Triton X-100 and spectra were taken as described for the dansyl chloride site. The transfer efficiency was found to be 0.85. The limiting anisotropy was 0.285 and the static anisotropy (at 23°C) was 0.240. These results imply a cone angle of 19°, a range of K^2 from 0.055 to 3.5, and a range of R_0 from 2.8 to 5.6 nm. Therefore the distance between retinal and dansyl-Glu-74/Asp-85 is between 2.1 and 4.2 nm (Table V).

Discussion

We have reported the characterization of two fluorescent labeling reactions of bacteriorhodopsin.

Dansyl chloride site

The product of reacting purple membrane with dansyl chloride is predominantly bacteriorhodopsin labeled at Lys-41 (Fig. 1). Step-wise recoveries at each step (Table I) are sufficient to make it extremely unlikely that another major labeling site could have been missed. We previously showed that no reaction occurs in the sequence region 72–248, and greater than 70% of the product is between residues 33 and 56 [12]. We initially inferred that the major dansyl chloride labeling site is at Lys-40, based on an erroneous report by Bridgen and Walker [36] that retinal is bound at Lys-41. To our surprise, sequence analysis showed no label at Lys-40 and all at Lys-41. In contrast to the report by Ovchinnikov [8] we see no evidence for labeling at Lys-30, although it is not possible to compare reaction conditions, since none are given in his brief review article. The two fractions of additional labeling that we previously reported [12], which amounted to 30% of the total, could consist of partially cleaved peptides (for example, residues 1–32). In this case, label could be at Lys-30, but we would not have seen it in the sequence analysis, since the N-terminal pyroglutamate does not react with phenylisothiocyanate. Alternatively, the additional fractions could be residues 33–56 with small modifications that would result in different mobilities on HPLC (for example, C-terminal homoserine lactone, or formyl serine [37]). We can set an upper limit on the labeling heterogeneity by assigning the two small labeled fractions observed by HPLC to label at Lys-40 and Lys-30. The largest of these two fractions contains approximately 17% of the label. Although we found some additional label non-covalently bound to the membrane (0.3 mol/mol) it is possible to remove this material by repeated washings and centrifugations.

Dansyl hydrazine site

This labeling reaction is not as specific as with dansyl chloride. We previously reported [13] that label is attached to carboxyl groups in the C-terminal tail, as well as at an internal sequence position(s). The stoichiometry of labeling is difficult to quantitate, due to the lability of the hydrazide linkage, but our present results (tail: 0.61 mol/mol; internal: 0.49 mol/mol) are in reasonable agreement with our previous report (tail: 0.73; internal: 0.35; [13]). We previously showed that the C-terminal label can be completely removed by treatment with papain. The remaining label is entirely on the large chymotrypsin fragment. It migrates near the cyanogen bromide peptide containing residues 72–118, CNBr 10, and appears to be derived from it (Fig. 3). Using cleavage at tryptophan and methionine, we found that most of the label migrates with small peptides (Fig. 4). This result shows that the label is predominantly at Glu-74 or Asp-85. Although as much as 10.7% of the label may be elsewhere on CNBr 10, it is unlikely to be at Asp-115, since we previously reported [28] that this site reacts with carbodiimides only under very restrictive conditions. Thus, although we have not fully located the dansyl hydrazine site(s), it is most likely on the 3rd helical segment of bacteriorhodopsin.

Proximity to retinal

There are formidable problems with energy

transfer measurements in the purple membrane system. In the intact membrane, the retinal chromophores are arranged in a hexagonal lattice of trimers with a spacing of 3.5 nm. Thus if retinal is used as an energy acceptor, any fluorescent probe on bacteriorhodopsin is likely to be quenched not only by the retinal in the same bacteriorhodopsin, but also by the adjacent ones. In order to simplify this problem, we solubilized the labeled membrane in Triton X-100 prior to fluorescence measurement. In Triton X-100, there is only one bacteriorhodopsin monomer per micelle [36]. A second difficulty is the large fluorescence anisotropy we observed for the labels. The high limiting anisotropies (0.204 for dansyl-Lys-41 and 0.285 for dansyl hydrazine-Glu-74/Asp-85) indicate that the dansyl groups are relatively immobile. Previous studies have shown that the retinal chromophores, the energy acceptors, are also rigid [38]. Dipole orientation strongly influences the efficiency of energy transfer. Only in the case of low anisotropy can be narrow distance range be calculated with any certainty from the measured transfer efficiency [34].

In view of the high anisotropy, only rather limited proximity questions may be asked. What is the minimum donor-acceptor distance compatible with the measured transfer efficiency? Does this distance place any constraints on models of the bacteriorhodopsin structure? The minimum distances between retinal and the dansyl side chains were estimated (Table V). We have attempted to correlate these distances with the electron density map of bacteriorhodopsin, in order to obtain some information about the relationship between the crystal structure and the amino acid sequence. The analysis is based on the following assumptions. (1) The fluorescence energy donors are at the membrane surfaces, which are smooth planes separated by 3.8 nm. (2) The transmembrane regions of bacteriorhodopsin are α-helix (25 residues). The helical segments of the amino acid sequence are those suggested by Huang et al. [5]. (3) The transition dipole of retinal is centered at 1.3 nm from the extracellular surface (Leder and Thomas, personal communication) and 2.5 nm from the cytoplasmic surface. The donor-acceptor distances can now be calculated in terms of distances projected on the plane of the membrane: 1.64 nm (Lys-41-retinal) ($1.64^2 = 2.99^2 - 2.5^2$) and 1.65 nm (Glu-74-retinal) ($1.65^2 = 2.1^2 - 1.3^2$). The minimum distance in projection is obtained assuming all the label is on Glu-74. If all label were on Asp-85, this would imply a larger projected distance for the measured transfer efficiency, since Asp-85 is thought to be about two helical turns into the membrane interior, placing it closer to retinal in the trans-membrane direction. The segment of peptide backbone to which the dansyl-lys-41 or dansyl-Glu-74 is attached is, on the average, within 0.6 nm of the center of the naphthalene ring (Lys-41 or Glu-74 side chain plus sulfonyl group and half the naphthalene ring of dansyl).

Labeling heterogeneity could affect these calculations significantly. A minor labeling site further from the energy acceptor than the major site would allow a closer minimum donor-acceptor distance for a given transfer efficiency. We have considered this possibility, using the equation:

$$E = f_1 R_0^6/(R_1^6 + R_0^6) + f_2 R_0^6/(R_2^6 + R_0^6) \quad (1)$$

where f_1 and f_2 are the fractions of sites 1 and 2, R_1 and R_2 are the donor-acceptor distances, E is the measured transfer efficiency, and R_0 is the minimum possible value for the 50% transfer distance, assuming the anisotropy is the same for both sites.

For the dansyl chloride site, possible secondary sites include Lys-40 and Lys-30. Minor occupation of the Lys-40 site would have essentially no effect on the calculated minimum donor-acceptor distance, since it is adjacent in the sequence to the major Lys-41 site and is also considered in most structure models to be on the same helix. Occupation of the Lys-30 site would be quite significant, since it is thought to be on a different helix. We assume that Lys-30 and Lys-41 are at the membrane surface and 1.0 nm apart (helix-helix spacing). In the geometry that would most decrease the minimum distance, R_1 (Lys-41) and R_2 (Lys-30) are hypotenuses of right triangles that share one side (2.5 nm) and for which the other sides are d (Lys-41) or $d + 1.0$ nm (Lys-30), where d is the distance of Lys-41 from retinal projected onto the membrane surface. Substituting into Eqn. 1, assuming 17% occupancy at Lys-30, gives a value of 1.48 nm for d. This contrasts with 1.64 nm calculated above.

For the dansyl hydrazine site, major labeling is at Glu-74 and/or Asp-85 (site 1) and minor labeling may be at Asp-96, 102 and/or 104 (site 2). The maximum effect of heterogeneity would be obtained by placing all of site 2 at the opposite side of the membrane from site 1. In this case, R_1 is the hypotenuse of a right triangle of sides 1.3 nm and d, and R_2 is the hypotenuse of a right triangle of sides 2.5 nm and d, where d is the donor-acceptor distance projected on the membrane plane. Solving Eqn. 1 with 10.7% of site 2 gives $d = 1.45$ nm, compared with 1.65 calculated assuming only one site.

Circles showing the minimum projected donor-acceptor distances are drawn on a projection of the bacteriorhodopsin structure based on the work of Seiff et al. [39] and Kouyama et al. [38] (Fig. 5). The center of the circles is positioned at the center of the retinal polyene. The positions of dansyl groups of dansyl-Lys-41 and dansyl-Glu-74/Asp-85 must lie outside the outer dashed circle in Fig. 5 (diameter 1.65 nm), in projection on the membrane plane. The α-carbons of position 41 and 74 must lie outside the inner dashed circle in projection. The energy transfer results for single sites clearly exclude helix 6 from being helix B, containing Lys-41, and they also exclude helix 6 from being helix C, containing Glu-74/Asp-85 (using the numbering and lettering scheme of Engelman et al. [3]: helices are lettered A–G from amino to carboxyl terminus, and they are numbered so that the projected helices as drawn in Fig. 5 are numbered 1–7 counterclockwise from the lower left). Considering labeling heterogeneity, helix B and C still cannot be helix 6, assuming a central location for the α-carbons of helix 6 within the projected electron density.

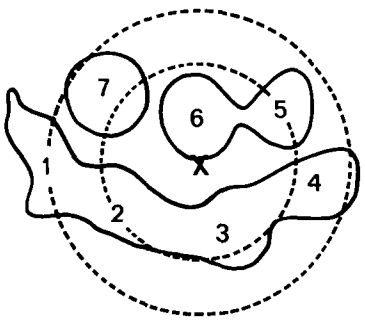

Fig. 5 Proximity of dansyl-Glu-74/Asp-85 and dansyl-Lys-41 to retinal. The position of the center of retinal polyene, from Seiff et al. [39], is marked X on a projection of bacteriorhodopsin structure with helices numbered 1–7 (Engelman et al. [3]). The outer dotted circle is the closest projected distance to retinal of either dansyl group allowed by fluorescence energy transfer data. The inner circle is the closest position permitted for α-carbon of Glu-74/Asp-85 and Lys-41.

We can now compare our measurements with conclusions drawn from other experiments that relate to the helix connection question. Dumont et al. [40] concluded that helix 6 is near helix B. Although the energy transfer results reported here appear to exclude helix 6 from being helix B, assignment of helix B to helix 2, 3, 4, 5 or 7 would be consistent with their observed Pt binding site. The assignment of helix G by Katre et al. [10] to helices 2, 3, 5 or 7, based on a Hg labeling site, is also compatible with our fluorescence results. Our experiments exclude 14 of the 41 most probable models of Engelman et al. [3] and 28 of the 42 models that Trewhella et al. [9] derived from neutron diffraction data. Seiff et al. [41] deuterated Lys-41 with phenylisothiocyanate and located the site by neutron diffraction. They concluded that helix B must be helix 3, 4, 5 or 6. Our results add a further constraint to the location of helix B, limiting it to 3, 4 or 5. Agard and Stroud [4] extended the Fourier analysis of Henderson and Unwin [2] to reveal surface features which they assigned to helix linker regions. They suggested five most likely models, two of which are excluded by our energy transfer data.

By applying all of the helix proximity data cited above to the Engelman, Trewhella and Agard-Stroud models, only six models survive: EDCABGF, ECBAGFD, DCBAGFE, DEBAGFC, FEDCBAG and FGEABDC. Only the first and the last two contain the G helix in a position compatible with the location of the Schiff base site proposed by Seiff et al. [39]. The last model seems particularly appealing, since it not only satisfies nearly all constraints but it also places the long BC and EF linker regions in positions that require long connections between non-adjacent helices.

Acknowledgments

We thank John Tuley for technical assistance, Charles Bittle for performing TLC analyses, Paul

Horowitz for fluorescence polarization measurements, Roberto Bogomolni for assistance with flash spectroscopy, Kamal Bitar for amino acid sequence analysis, and Kathy Wall for amino acid analyses. R.R. thanks Walther Stoeckenius for this kind hospitality at the Cardiovascular Research Institute, University of California at San Francisco. This work was supported by grants from NIH (GM 25483 and RR 08194), NSF (PCM 7822732) and the Robert A. Welch Foundation (AX-736 and AX-1040).

References

1 Stoeckenius, W. and Bogomolni, R. (1982) Annu. Rev. Biochem. 52, 587–616
2 Henderson, R. and Unwin, N. (1975) Nature (Lond.) 257, 28
3 Engelman, D., Henderson, R., McLachlan, A. and Wallace, B. (1980) Proc. Natl. Acad. Sci. USA 77, 2023–2027
4 Agard, D. and Stroud, R. (1982) Biophys. J. 37, 589–602
5 Huang, K., Liao, M., Gupta, C., Royal, N., Biemann, K. and Khorana, H. (1982) J. Biol. Chem. 257, 8596–8599
6 Steitz, T., Goldman, A. and Engelman, D. (1982) Biophys. J. 37, 124–125
7 Kyte, J. and Dootlittle, R. (1982) J. Mol. Biol. 157, 105–132
8 Ovchinnikov, Yu. (1982) FEBS Lett. 148, 179–191
9 Trewhella, J., Anderson, S., Fox, R., Gogal, E., Khan, S., Engelman, D. and Zaccai, G. (1983) Biophys. J. 42, 233–241
10 Katre, N., Finer-Moore, J. and Stroud, R. (1984) Biophys. J. 46, 195–204
11 Jap, B.K., Maestre, M., Hayward, S. and Glaeser, R. (1983) Biophys. J. 43, 81–89
12 Harris, G., Renthal, R., Tuley, J. and Robinson, N. (1979) Biochem. Biophys. Res. Commun. 91, 926–931
13 Renthal, R., Dawson, N., Tuley, J. and Horowitz, P. (1983) Biochemistry 22, 5–12
14 Wu, C.W. and Stryer, L. (1982) Proc. Natl. Acad. Sci. USA 69, 1104–1108
15 Renthal, R., Steinemann, A. and Stryer, L. (1973) Exp. Eye Res. 17, 511–515
16 Oesterhelt, D. and Stoeckenius, W. (1974) Methods Enzymol. 31, 667
17 Gerber, G., Anderegg, R., Herlihy, W., Gray, C., Biemann, K. and Khorana, H. (1979) Proc. Natl. Acad. Sci. USA 76, 227–231
19 Kates, M. (1972) Techniques of Lipidology, pp. 436–437, Elsevier, Amsterdam, New York
20 Huang, K., Bayley, H. and Khorana, H. (1980) Proc. Natl. Acad. Sci. USA 77, 323–327
21 Lozier, R., Bogonolmi, R. and Stoeckenius, W. (1975) Biophys. J. 15, 955–62
22 Ozols, J. and Gerard, C. (1977) J. Biol. Chem. 252, 5986–5989
23 Khorana, H.G., Gerber, G., Herlihy, W., Gray, C., Anderegg, R., Nihei, K. and Beimann, K. (1979) Proc. Natl. Acad. Sci. USA 76, 5046–5050
24 Renthal, R., Harris, G. and Parrish, R. (1979) Biochim. Biophys. Acta 547, 258–269
25 Renthal, R. (1981) J. Biol. Chem. 256, 11471–11476
26 Stryer, L. (1965) J. Mol. Biol. 13, 482–495
27 Melhuish, W. (1973) Natl. Bur. Stand. Spec. Publ. 378, 137–150
28 Renthal, R., Cothran, M., Espinoza, B., Wall, K. and Bernard, M. (1985) Biochemistry 24, 4275–4279
29 Renthal, R. (1981) Biophys. J. 33, 173a
30 Renthal, R. and Wallace, B. (1980) Biochim. Biophys. Acta 592, 621–625
31 Stryer, L. (1978) Annu. Rev. Biochem. 47, 819–846
32 Reynolds, J. and Stoeckenius, W. (1977) Proc. Natl. Acad. Sci. USA 74, 2803–2804
33 Casadio, R. and Stoeckenius, W. (1980) Biochemistry 19, 3374–3381
34 Renthal, R. (1977) Biochem. Biophys. Res. Commun. 77, 155–161
35 Kawato, S., Kinosita, K. and Ikegami, A. (1977) Biochemistry 16, 2319–2324
36 Bridgen, J. and Walker, I. (1976) Biochemistry 15, 792–798
37 Tarr, G. and Crabb, J. (1983) Anal. Biochem. 131, 99–107
38 Kouyama, T., Kimura, Y., Kinosita, K. and Ikegami, A. (1982) J. Mol. Biol. 153, 337–359
39 Seiff, F., Wallat, I., Ermann, P. and Heyn, M. (1985) Proc. Natl. Acad. Sci. USA 82, 3227–3231
40 Dumont, M., Wiggins, J. and Hayward, S. (1984) Proc. Natl. Acad. Sci. USA 78, 2947–2951
41 Seiff, F., Wallat, I., Westerhauser, J. and Heyn, M. (1986) Biophys. J. 49, 210a